Catena 180 (2019) 41–54

Contents lists available at ScienceDirect

Catena

journal homepage: www.elsevier.com/locate/catena

Pioneer plant *Phalaris arundinacea* and earthworms promote initial soil structure formation despite strong alluvial dynamics in a semi-controlled field experiment

A. Schomburg[a,b,*], P. Brunner[b], P. Turberg[c,d], C. Guenat[c,d], M. Riaz[e,f], R.C. Le Bayon[a], J. Luster[e]

[a] *Functional Ecology Laboratory, Institute of Biology, University of Neuchâtel, Switzerland*
[b] *Center for Hydrogeology and Geothermics (CHYN), University of Neuchâtel, Switzerland*
[c] *Laboratory of Ecological Systems – ECOS-EPFL, Ecole Polytechnique Fédérale de Lausanne (EPFL), Switzerland*
[d] *Swiss Federal Institute for Forest, Snow and Landscape Research WSL, Site Lausanne, Switzerland*
[e] *Swiss Federal Institute for Forest, Snow and Landscape Research WSL, Site Birmensdorf, Switzerland*
[f] *Department of Environmental Sciences & Engineering, Government College University, Faisalabad 38000, Pakistan*

ARTICLE INFO

Keywords:
Sediment deposition
Soil evolution
Flooding
River restoration
Freeze core
X-ray analysis

ABSTRACT

Soil structure formation is among the most important processes in river floodplains which are strongly influenced by alluvial dynamics. In the context of river restoration projects, a better understanding of soil structure formation in habitats adjacent to the river can help to prevent damages caused by riverbank erosion. Ecosystem engineers such as pioneer herbaceous plants and earthworms likely contribute to soil structure formation even despite less favourable environmental conditions. This study aims to assess the capacity of the herbaceous perennial and native species *Phalaris arundinacea* and earthworm communities to promote a stable soil structure in alluvial sediments, in particular fresh alluvial deposits, in the short term. Delimited plots were set-up in a restored floodplain adjacent to the Thur River in NE Switzerland and exposed to natural alluvial dynamics for 19 months. Four treatments were replicated in a randomised complete block design: (i) plots with *Phalaris arundinacea* as only vegetation, (ii) plots with all vegetation constantly removed, (iii) and (iv) the earthworm community reduced by mustard treatment, otherwise as (i) and (ii), respectively. Soil structure formation was analysed at the end of the experiment using different indicators: aggregate stability, field-saturated hydraulic conductivity and the porosity calculated from X-ray CT reconstructions of freeze cores. *Phalaris arundinacea* was capable of improving the porosity and aggregate stability of both alluvial sediments present at the beginning of the experiment but also of sediments freshly deposited during the observation period. The latter indicates a structuring effect within only one vegetation period. Earthworm abundance was as a whole very low, most likely due to the large proportion of sand. There was a small earthworm effect on soil structure formation, and only in combination with *Phalaris.arundinacea*. Our findings highlight the ability of *Phalaris arundinacea* in efficiently structuring sandy alluvial sediments in the short term even under strong alluvial dynamics. *Phalaris arundinacea* can therefore play a key role in the early stage of river restoration projects. Thus, facilitating the colonisation by such native pioneer herbaceous plants is a suitable step to improve the success of river restoration projects.

1. Introduction

Interactions between hydrologic and pedologic processes strongly control ecosystem services and the ecological balance in semi-terrestrial systems. In the past, these processes were investigated within their specific research domain and without considering the feedback mechanisms (Ma et al., 2017). For instance, soil development, e.g. the formation of a stable soil structure can be accelerated, inhibited or altered by hydrologic processes (Lin et al., 2005, 2015; Bätz et al., 2015; Schomburg et al., 2018). Soil structure formation is especially important in ecosystems that are constantly rejuvenated through exogenous dynamics, such as floodplains (Guenat et al., 1999; Bullinger-Weber et al., 2012; Mardhiah et al., 2014). In the course of alluvial dynamics, unconsolidated shore sediments can be eroded and/or deposited along the river bank that bury the existing soils (Gurnell and Petts, 2006; Greenwood et al., 2013; Gianni et al., 2016; Partington et al., 2017). Improving the structural stability of floodplain soils is required with regard to today's river management policies in several

* Corresponding author at: Functional Ecology Laboratory, Institute of Biology, University of Neuchâtel, Switzerland.
E-mail address: andreas.schomburg@unine.ch (A. Schomburg).

https://doi.org/10.1016/j.catena.2019.04.001
Received 7 November 2018; Received in revised form 13 February 2019; Accepted 4 April 2019

countries, including Switzerland. For much of the past 150 years, rivers have been cannelised in reaction to the need to protect anthropogenic settlements from floods and to the rising demand for suitable agricultural land, caused by the large growth of the population (Bundesamt für Umwelt BAFU, 2008, 2017). During the last two decades, river management strategies have slowly shifted from prioritising human requirements towards ecological aspects (Malmqvist and Rundle, 2002; Tockner and Stanford, 2002). Management goals were defined, among others, for the restoration of floodplains as biodiversity hotspots (Naiman and Décamps, 1997; Malmqvist and Rundle, 2002), and for the creation of inundation areas reducing the flood risk in settlement areas (Bundesamt für Umwelt BAFU, 2015). In the course of these river restoration projects, river channels should be widened and embankments removed. Floodplains adjacent to restored rivers are, in contrast to those next to cannelised ones, often subject to severe inundations. Besides river shore erosion and depostion of alluvial sediments, recurring floods can modify the hydraulic properties of alluvial deposits through rearranging particles and clogging macro-pores thereby increasing surface runoff (Bottinelli et al., 2010; Greenwood et al., 2013). On one hand, these processes can lead to strong alterations of the floodplain itself, such as land gain/loss (Junk and Welcomme, 1990) or the introduction of non-native plants (Hayashi et al., 2011), or threaten anthropogenic infrastructure downstream through obstruction of water ways and drainage ditches (Acreman et al., 2003). On the other hand, frequent flooding impedes the development of stable conditions in floodplain habitats and thus the natural succession of species (Bätz et al., 2015; Graf-Rosenfellner et al., 2016). A soil structure, stabilised by a spatial arrangement of macro-pores and aggregates composed of mineral and organic particles (Tisdall and Oades, 1982; Brussard and Kooistra, 1993), promotes stable conditions in floodplain habitats by reducing soil erosion (Diaz-Zorita et al., 2002; Velasquez et al., 2007; Mardhiah et al., 2014) and facilitating water infiltration (Ehlers, 1975; Pérès et al., 1998). The entanglement of smaller micro-aggregates of microbial origin into water-stable macro-aggregates is a process particularly involving soil macro-biota (Tisdall and Oades, 1982; Brown et al., 2000; Six et al., 2002; Kong and Six, 2010). In ecosystems of temperate latitudes, plants and earthworms act as soil engineers and can strongly contribute to soil structure formation by creating water-stable macro-aggregates (Lavelle et al., 1997; Tanner, 2001; Blouin et al., 2013). Aggregates formed by plants are physically compressed during root network extension and/or cemented by root exudates and associated rhizobacteria (Degens et al., 1994; Angers and Caron, 1998; Czarnes et al., 2000). Earthworms stabilise aggregates by mixing mineral and organic material during burrowing and casting and agglutinate ingested particles with mucus and saliva upon passage through their digestive tract (Blanchart et al., 1997; Brown et al., 2000; Lavelle and Spain, 2001). Along with aggregate formation, hydraulic properties of the soils can positively affect water infiltration and reduce surface water runoff (Gurnell and Petts, 2006). Moreover, a branched and robust network of earthworm tunnels can reduce soil erosion rates by > 50% (Shuster et al., 2002; Shipitalo et al., 2004; Jouquet et al., 2011). Pioneer plants and earthworms have the potential to improve the soil structural stability of floodplain soils. Pioneer plants generally show a large physical resistance to alluvial dynamics (Gurnell and Petts, 2006; Gurnell, 2014; Bätz et al., 2014), whereas earthworms tolerate waterlogging conditions in the soil for several weeks through physiological adaptations (Plum and Filser, 2005; Le Bayon et al., 2013, 2017). In the course of current river restoration projects, willows (*Salix* ssp.) are commonly planted to stabilise the riverbanks, as they grow relatively fast, are well adapted to alluvial dynamics, and are highly efficient in trapping sediments with their roots and thus promoting soil aggregation (Gurnell and Petts, 2002; Crouzy and Perona, 2012; Perona et al., 2012). Willows can help to establish post-pioneer riparian forests in habitats flooded every 2–3 years (Corenblit et al., 2009). On the other hand, stronger alluvial dynamics in close proximity to the river retard the engineering effect of willows (Gurnell, 2014; Bätz et al., 2014, 2015) and require a more efficient contribution to soil structure formation. Fast-growing herbaceous pioneer plants, such as *Phalaris arundinacea* and earthworms might be more competitive and promote initial soil structure formation. Such a short-term engineering effect would need to comprise the ability to improve the aggregate stability, the macroporous network and the hydraulic properties of sediments to which they are exposed and of sediments which are deposited during frequent flood events. However, characterising soil structure formation under such conditions in the field is challenging, as the abundance of plants and earthworms and the accumulation or loss rates of sediments are highly variable in space and time. Moreover, micro- and mesocosm experiments are suitable to determine the efficiency of each individual organism on soil structure formation, but the effects of strong alluvial dynamics cannot be accurately reproduced. A possibility is to install semi-controlled plots in the field and expose them to natural floods. This innovative approach combines the strengths of field and laboratory experiments, as the treatments can be controlled and develop dynamically under natural alluvial dynamics. However, patterns of soil structure formed by plants and earthworms are difficult to analyse in unconsolidated sandy soil material generally found in close proximity to the river (Walling and Collins, 2016; Liu et al., 2018), as the soil structure may collapse when applying conventional soil coring. Liernur et al. (2017) demonstrated freeze coring coupled with X-ray computed tomography (X-ray CT) as a non-destructive method well suited for the analysis of the soil structure in low-cohesive soils. Freezing of the soil matrix largely preserves the soil's structural integrity except for the matrix adjacent to the freezing lance (Humpesch and Niederreiter, 1993; Franchini and Zeyer, 2012; Liernur et al., 2017). Recently, X-ray CT has been used to determine soil structure formation through the analysis of the soil's macro-porosity, as well as the length, volume and connectivity of root galleries and earthworm tunnels (e.g. Capowiez et al., 2011, 2015; Amossé et al., 2015). The aim of this study is to analyse the short-term effects of the pioneer herbaceous plant *P. arundinacea* and earthworms on soil structure formation of alluvial sediments and recent deposits under strong alluvial dynamics, e.g. flooding, erosion and deposition of sediments. To this end, we exposed delineated plots containing treatments of *P. arundinacea* and earthworms to the alluvial dynamics in a restored river floodplain and assessed the short-term soil structure formation by means of innovative methods, e.g. freeze coring and X-ray CT over a period of 19 months. We hypothesise that pioneer vegetation and earthworms contribute to initial soil structure formation in the alluvial sediments and recent deposits by improving their macro-porosity, structural stability and hydraulic properties during this short period.

2. Materials & methods

2.1. Experimental design

The field experiment was conceptualised as a randomised complete block design (Fig. 1). Four different treatments were set up in plots with two replicates assigned to each of three blocks ($4 \times 2 \times 3 = 24$ plots in total). The assignment of treatments to the plots differed from one block to another (Fig. 1). Four different treatments were designed: 1) with *P. arundinacea*, with earthworms (+P+EW), 2) with *P. arundinacea*, without earthworms (+P−EW), 3) without *P. arundinacea*, with earthworms (−P+EW), and 4) without both *P. arundinacea* and earthworms (−P−EW). Sampling and on-site experiments were performed at different depths that were defined specifically for each method. This allowed data analysis at different layouts: i) one and two-factor analyses for data available at the block level (earthworm community, effect analysis of plants and earthworms on sediment accumulation), and ii) analysis of data available for treatments and depths.

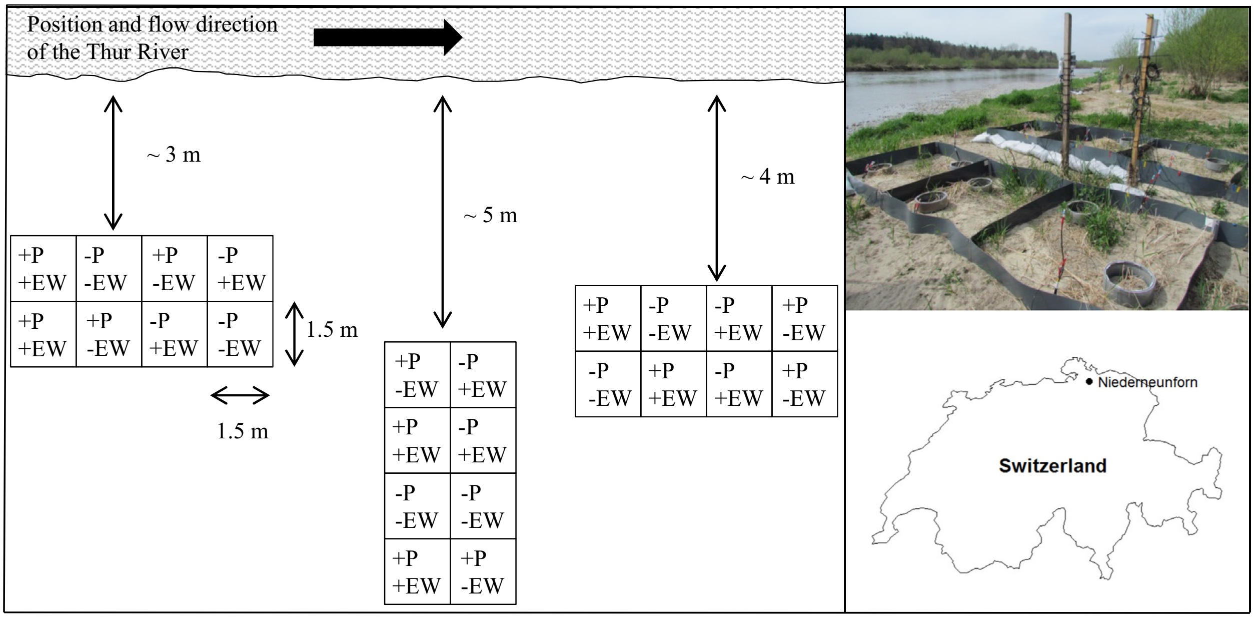

Fig. 1. Schematic spatial arrangement of the field experiment at the Schaffäuli site along the Thur River. Altitude was approximately 373.5 m a.s.l. P stands for *P. arundinacea* and EW for earthworms. Example picture of block nr. 2 and the location of the site in Niederneunforn, Switzerland.

2.2. Construction and maintenance of field plots

In February/March 2015, plots were installed in close proximity to the Thur River (3–8 m at a discharge rate of 46.8 $m^3 s^{-1}$ corresponding to the yearly average) at the Schaffäuli site (Fig. 1), located in NE Switzerland close to Niederneunforn (NNF, 8°77′12″ E, 47°59′10″ N). The Schaffäuli site represents the largest current river restoration project in Switzerland (Schirmer et al., 2014). A 2 km long section of the river was restored in 2002 by removing the embankments. Since then, strong alluvial dynamics have led to several inundations each year of the adjacent floodplain and caused erosion and deposition of unconsolidated alluvial sediments. Inundations are of natural origin, as the Thur River is not regulated by any artificial reservoirs along its course of 130 km. Due to a nivo-pluvial hydrologic regime, floods principally occur in late spring during snow melt and in late summer after heavy rainfall in the catchment area (Fournier et al., 2013). The plots were installed in a zone which was sparsely colonised by pioneer vegetation due to frequent floods in summer 2014 and in January 2015. *Phalaris arundinacea* was the predominant herbaceous soil engineering plant, other abundant species were *Urtica dioica* and the non-native species *Impatiens glandulifera*. Total thickness of the sediments at the installation site, that had been accumulated since the widening of the river in 2002, was around 80 cm at the beginning of the experiment. Each plot measured 1.5 × 1.5 m, and was delimited by PVC walls extending to a soil depth of 40 to 50 cm and to about 10 cm above the soil surface at the time of installation. PVC walls minimised root extension, prevented migration of earthworms into or from adjacent plots and the surrounding sediments and promoted the accumulation of sediments within each plot. Treatments were initially created and maintained through the periodic removal of either plants or earthworms (removal experiment). For devegetated plots, shoots of all plants were removed by trimming biweekly in 2015 and 2016 except during the winter season, and for plots with vegetation, the shoots of all plants except *P. arundinacea* were removed. Also during the vegetation periods, *P. arundinacea* shoots cut from outside of the experimental plots were applied in equal amounts to all plots without vegetation every two months and after each major flood, in order to provide a nutrient resource for earthworms and to minise differences in evaporation from plots with and without vegetation. The abundance of earthworms was reduced by using the hot-mustard extraction method, described in Lawrence and Bowers (2002), in May and October 2015. After pre-moistening the soil by extensive sprinkling with river water, two 24 L portions of a suspension of 6% pre-soaked mustard seeds in river water were applied with a watering can. Earthworms appearing at the soil surface during 15 min between the two mustard applications and within 30 min after the second application were collected and preserved in 70% ethanol for later identification. Finally, the plots were again extensively rinsed with river water. The latter was also done for all plots without mustard treatment. Once set up, the experiment was exposed to the natural alluvial dynamics for 19 months. After each flood event, the thickness of the sediment accumulation and the rate of erosion was estimated by measuring the distance between soil surface and the upper rim of the separations walls at 12 locations inside each plot. Sediment loss and gain rates were averaged to one value for each plot. The magnitude of each flood event was determined based on the maximum daily discharge, which was monitored at the Niederneunforn gauging station at 5 min intervals 500 m downstream of the site (Canton Thurgau river gauging station no: F2900, coordinates: 8°46′57.78″ E, 47°35′20.76″ N, altitude: 372 m a.s.l.). Additionally, groundwater levels were monitored at a 30-minute interval by using a piezometer which was installed in close proximity to the plots. The data logger was out of service in the period between the 08.04.2015 and the 15.05.2015. However, discharge data from the Niederneunforn gauging station did not indicate any obvious groundwater level rise during this period. The experiment ended in October 2016 after 19 months of exposure with a final sampling of plants and earthworms, and conducting soil analyses. *P. arundinacea* was cut and dried at 65 °C for 48 h. In addition, plant litter was collected from each plot (naturally produced litter on plots with vegetation, and the one remaining from the last addition on plots without vegetation), dried and weighed. The abundance of earthworms was assessed for all plots using the same application as described above. The method was applied to three standard-size subplots (0.5 × 0.5 m) per plot, using standard amounts of 6% mustard suspension in river water, i.e. 2 portions of 5 L per subplot. Subsequently, handsorting was applied on a 0.2 × 0.2 square in the center of each subplot. Earthworms were weighed individually, identified at species level following the identification key of Blakemore (2008) and assigned to its ecological category (Bouché, 1972). Unidentifiable juveniles were just grouped and weighed.

2.3. Hydraulic properties

The infiltration capacity of the soil was measured using a Guelph Permeameter (model 2800K1, Soilmoisture Equipment Corporation) (Reynolds and Elrick, 1985). Two measurements were performed per plot, one at 10 cm and one at 30 cm depth. The aim was to perform one measurement in a sediment which was deposited during the experimental period and another one in a sediment deposited before the experiment was set up. Cylindrical holes of 3 cm radius were prepared for each measurement in the respective depths using an auger, and water-saturated before starting the infiltration test. The double-head method was applied for each hole, i.e. one measurement was conducted with a first head hight of 5 cm (*H1*) and a second head hight of 10 cm (*H2*) (Reynolds et al., 2002). The scale was read at the inner reservoir of the device. Fall rate was noted in intervals of 30 s until a steady state fall rate was reached after four identical consecutive measurements. The field saturated hydraulic conductivity (K_{fs}) was calculated from the infiltration tests according to the Eqs. (1)–(5) (Appendix A) (Reynolds et al., 2002). In case that the results of the double head method showed invalid, i.e. negative values for K_{fs}, calculations were performed according to the single head method separately for both head heights using Eq. (6) (Appendix A) and the results were averaged (Reynolds et al., 2002).

2.4. Soil monolith excavation

One soil monolith from each plot was excavated using the freeze core method described in Humpesch and Niederreiter (1993). For this purpose, a tubular metal lance of 50 cm in length and 4 cm in diameter, in which a spiral pipe was installed and which was hollow in the center, was used. The metal lance was carefully hammered into the soil at an undisturbed location in each plot (i.e. without installed sensors and not too close to a PVC wall to avoid edge effects). 30 L of liquid nitrogen were continuously injected over 45 min into the spiral cooling down the metal lance. During this period, the surrounding soil matrix froze around the lance via thermal conductivity. Immediately afterwards, the core was mechanically excavated using a hydraulically controlled crane fixed by a tripod (Fig. 2a). The metal lance was subsequently melted from the core with a heating stick which was inserted into the hollow. Freeze cores were stored in styrofoam boxes at −20 °C for further treatments.

2.5. X-ray CT analysis

Freeze cores were prepared for X-ray computed tomography (X-ray CT) by storing them in cylindrical PVC tubes of 35.5 cm in diameter, 65 cm in height and 0.8 cm in thickness which were closed at both ends (Liernur et al., 2017). The remaining space between the freeze core and the PVC tube was filled with styrofoam chips in order to prevent movements of the core during the scanning process. A LightSpeed VCT (GE Medicalm Systems) medical scanner was used for the scanning. The scanner rotates around the PVC tube and emits X-ray beams on a 1.2 mm focal spot reaching a peak energy of 120 keV and a tube current of 500 mA. Data were acquired by a 64 channel detector and an axial pitch of 0.625 mm. Recent X-ray CT analyses of freeze cores and soil mesocosms were already performed using the same settings (Turberg et al., 2014; Amossé et al., 2015; Liernur et al., 2017). Image projection of the sequence was defined on a grid of 512 × 512 pixels and adapted to the transaxial field of view. This led to a voxel size of in average 0.55 × 0.55 × 0.3 voxels per image. Treatment of the raw images was performed using the programs imageJ (Schneider et al., 2012) and Avizo version 9.3.0 (FEI, 2016) (Fig. 2b). Cylindrical substacks of image sequences were produced in ImageJ based on the predefined depth of soil samples (see Section 2.6). In a second step, substacks of the recent alluvial deposits were created according to the thickness measured after their deposition. Image sequences of each substack were afterwards implemented in Avizo. The void representing the macro-pores formed by cracks and macro-biological activity was separated from the mineral and organic matrix applying a binarisation. Binarisation was performed using the default Otsu-algorithm (Otsu, 1979) which was already applied to determine the void of soil matrices in recent studies (Iassonov et al., 2009; Liernur et al., 2017) (Fig. 2c). The macro-porosity of the matrix was analysed using the material statistics function provided in Avizo which calculates the void/matrix ratio of each image slide. Afterwards, a skeleton of the binarised data was produced by the auto-skeleton function allowing the total number and length of the segments and the number of nodes to be calculated. An estimation of the pore connectivity was calculated as the ratio between the number of segments and the number of nodes. However, pushing the metal lance into the soil significantly affects the structural integrity of the freeze cores (Strasser et al., 2015; Liernur et al., 2017). Therefore, a buffer zone around the metal lance needed to be defined, in order to consider only the undisturbed matrix for the analyses. The image-set of each core was visually checked for anisotropic lines, indicating a compaction or displacement of the matrix along the metal lance. The area containing anisotropic lines was excluded from the analysis by defining a cylindrical buffer area around the metal lance (Fig. 2d). This buffer area was defined individually for each substack of an image sequence, ranging from 1.8 to 3.2 cm distance from the metal lance.

2.6. Additional soil sampling

Using an auger, soil samples were collected from three chosen locations within each plot at the following depths: 0–7.5 cm, 7.5–22.5 cm, 22.5–37.5 cm and 37.5–52.5 cm. The depth 0 was defined as the top surface at the start of the experiment. Sediments deposited during the observation period were not sampled. For each plot, the samples taken at the same depth were pooled for later analysis. Texture of the composite soil samples was determined using the pipette method (Gee and Bauder, 1986). Soil aggregates were collected in the same four predefined depths. Since freezing and thawing of a soil matrix can break down soil aggregates and reorientate soil particles, soil samples were not directly taken from the freeze cores (Singer et al., 1992; Dalal and Bridge, 1996). Aggregate stability was analysed by determining the proportion of water-stable macro-aggregates which is a classic and robust indicator for estimating soil structural stability (Six et al., 2000). Macro-aggregates between 250 and 2000 μm size were considered and plunged into demineralised water for 5 min (Kemper and Rosenau, 1986) using an automatic sieve-immersion apparatus described in Murer et al. (1993).

2.7. Statistical data processing

Data were processed using different implementations of analyses of variance (ANOVA) and adapted to the layout of the experiment. Earthworm data were analysed using a one-way ANOVA. Effect analyses of *P. arundinacea* and earthworms on the thickness of sediment accumulations during the 1.5 years exposure period were performed using a two-way ANOVA for 2 × 2 factorial designs. The variability of the field-saturated hydraulic conductivity, total segment length, porosity and pore connectivity within the treatments and the depths of the plots were analysed using ANOVAs for randomised complete block designs. The variability of the field-saturated hydraulic conductivity, total segment length, porosity and pore connectivity were defined as response variables. The treatments and the depths were set as predictor variables. The predictor “treatment” had four levels (+P−EW, −P +EW, +P+EW, −P−EW) and the predictor “depth” had four levels for the analysis of precedent sediments (0–7.5 cm, 7.5–22.5 cm, 22.5–37.5 cm, 37.5–52.5 cm) and three levels for the analysis of recent alluvial sediments deposited during the observation period (sediment deposit summer 2016, sediment deposit 21.11.2015, initial sediment). Since the experimental design was not orthogonal, ANOVAs were

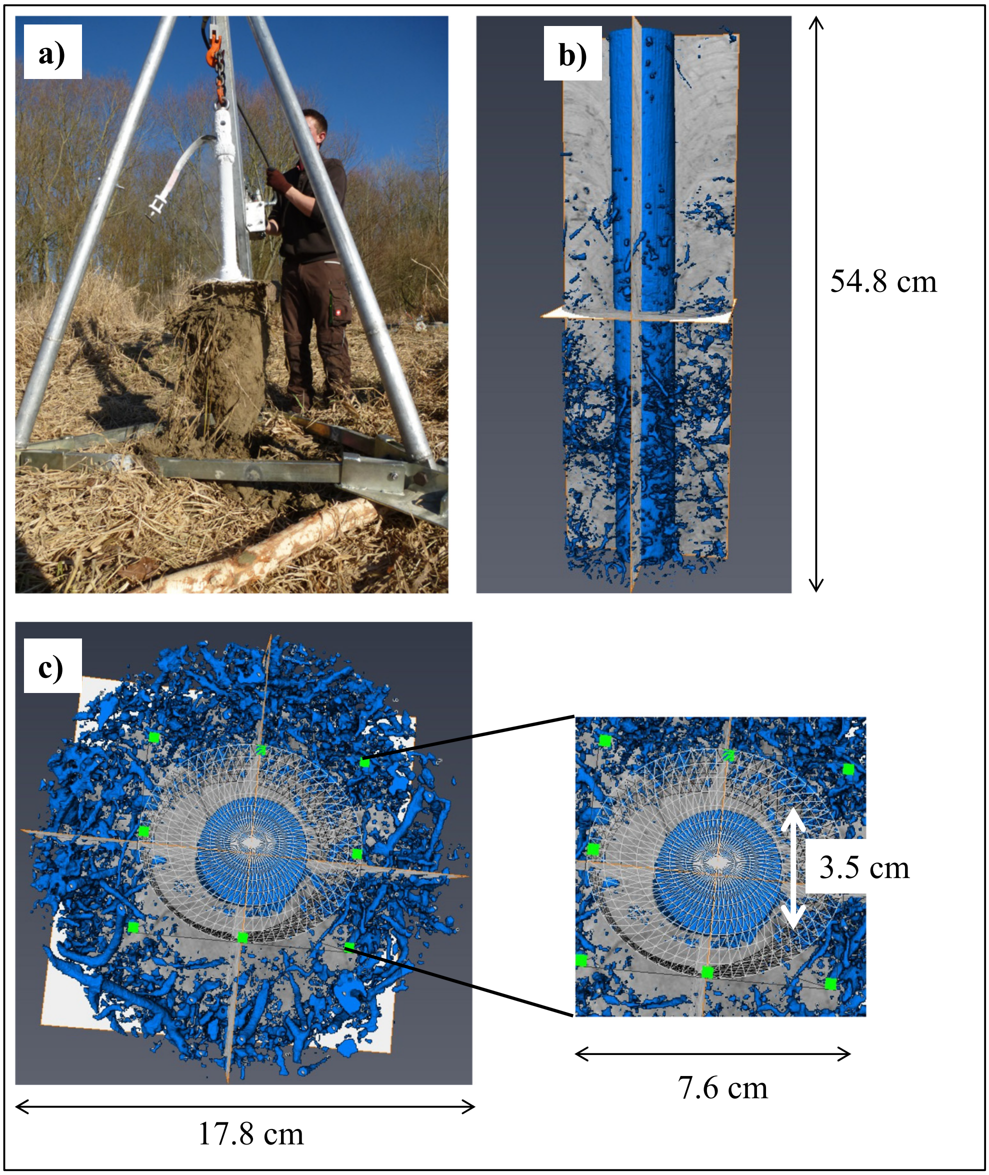

Fig. 2. Freeze core excavation in the field a), and image analysis of X-ray CT scans. b) Shows the binarisation of a substack volume according to the Otsu algorithm for automatic thresholding. Identified voids which were separated from the mineral matrix are shown in blue. c) Shows the cylindrical buffer zone around the metal lance which was defined visually. Matrix and voids located inside the cylindrical mesh were not considered for porosity analysis. (For interpretation of the references to colour in this figure legend, the reader is referred to the web version of this article.)

calculated using the sum of squares type III. Prior to the analyses, requirements for normality and homoscedasticity were checked by means of the Shapiro-Wilk test and the Bartlett test. As the total segment length failed the criteria for normality, data were logarithmised prior to the ANOVA. Post-hoc analyses at the main factor levels were performed using Tukey's HSD test. Hypotheses were tested at an $\alpha = 0.05$ significance level, accepting the risk at a p-value < 0.05. Statistical analyses and data visualisations were conducted in R version 3.5.1 (R Core Team, 2013) using the packages “easyanova” (Arnhold, 2013) for ANOVAs, as well as “ggplot2” (Wickham, 2009) and “gridExtra” (Auguie, 2016) for graphs.

3. Results

3.1. Alluvial dynamics

During the 19 months of exposure period, four flood events occurred leading to a considerable deposition of alluvial sediments (Table 1): largest sediment depositions resulted from the flood occurring on 21.11.2015 (on average 8.1 cm). Three consecutive events in summer 2016 led to smaller sediment accumulations, despite higher discharge rates. Only during the event in november 2015, sediment deposition varied within the treatments: in plots containing *P. arundinacea*, significantly larger amounts of sediment were deposited compared to the other treatments. (p-value < 0.05) (Table 1). In addition, plots were completely waterlogged during three more days (30.03.2015, 01.06.2015 and 31.01.2016) by rising groundwater levels (Fig. 3) As the plots were not flooded by incoming surface water at these three dates, no further sediments were deposited.

3.2. *P. arundinacea* and earthworms

Mean biomass of *P. arundinacea* in +P−EW plots was 2123 $g\,m^{-2}$. In the presence of earthworms, the biomass of *P. arundinacea* (mean value of 1968 $g\,m^{-2}$) was moderately reduced, but the effect was however not significant (Fig. 4a). Mean litter biomass was similar for

Table 1
Accumulation of sediment deposits at four sedimentation events (± SE) in cm for each treatment. P stands for *P. arundinacea*, EW for earthworms. Omnibus effects represent results of the Two-way ANOVA comparison test at an $\alpha = 0.05$ significance level accepting the risk at a p-value < 0.05. n.s. denominates non-significant effects. *P. arundinacea*:earthworm represents interaction effects between the vegetation and earthworms.

Date of sediment deposit	Max. discharge $[m^3 s^{-1}]$	Thickness of the sediment deposit according to treatments [cm] ± SE				Omnibus effects		
		+P−EW	−P+EW	+P+EW	−P−EW	*P. arundinacea*	Earthworm	*P. arundincea*:earthworm
21.11.2015	554	8.6 ± 1.7	6.1 ± 1.3	10.2 ± 2.1	4.8 ± 1.4	p < 0.05	n.s.	n.s.
13.05.2016	633	6.1 ± 0.9	3.2 ± 0.5	6.1 ± 1.5	4.9 ± 1.4	n.s.	n.s.	n.s.
17.06.2016	715	4.1 ± 0.7	3.3 ± 0.8	4.1 ± 0.7	3.5 ± 1.1	n.s.	n.s.	n.s.
05.08.2016	516	0.9 ± 0.3	1.6 ± 0.3	0.9 ± 0.3	0.9 ± 0.3	n.s.	n.s.	n.s.

+P+EW and +P−EW (mean values around 220 g m^{-2}) (Fig. 4b). Thus, the removal of earthworms did not have any significant effect on the litter biomass. Almost 75% of the earthworms found in the treatments were juveniles. More than 80 % of the juveniles could not be assigned to their ecological category, especially for anecic and epigeic species for which juveniles were almost indistingushable. Total abundance and biomass of earthworms were 2.5 times higher in the +P +EW treatment than in the treatments without vegetation (Table 2). Results were similar for the total number of juveniles, but not for adults. Proportions for ecological groups did not vary significantly between the treatments, except for juvenile-anecics and adult-endogeics (Table 2).

3.3. Hydraulic properties of the soil

Values for field saturated hydraulic conductivity were between 8.45e^{-4} and 2.49e^{-6} cm s^{-1} and indicated a large variability within the main factor levels of “treatment” and “depth” (Fig. 5). There were no significant single effects of “treatment” and “depth” to explain the variability of the field saturated hydraulic conductivity. Interaction effects were not significant either.

3.4. Soil texture and aggregate stability

Soil texture class was similar among the plots and was identified as loamy sand (IUSS Working Group WRB, 2006). Mean proportions were 78.96 ± 5.95% for sand, 14.67 ± 4.96% for silt and 6.37 ± 1.40% for clay. Soil texture did not show any significant correlation to the values for aggregate stability in this study (p-value < 0.6, $r_{pearson} = 0.045$). Thus, soil texture could be omitted as a predictor variable in the effect analysis. Nevertheless, soil texture indicated a depth gradient with an increasing proportion of the sand fraction and a decreasing proportion of the clay fraction in the topsoil (not shown). The contribution of “depth” to explain the variablility of aggregate stability was highly significant ($p < 0.001$) (Table 3). On the other hand, there was no significant “treatment” effect. The effect of the interaction between “treatment” and “depth” was not significant either, but the p–value ($p = 0.07$) was close to the threshold level of acceptance. Therefore, multiple comparisons at the main factor levels were nevertheless performed. Within the levels of “depth”, aggregate stability was lowest in 37.5–52.5 cm, increasing gradually to the soil surface. Regarding interaction terms, aggregate stability was significantly higher in the +P−EW treatment in the uppermost layer compared to the undermost layer. Values for the layers between 7.5 and 37.5 cm ranged in between (Fig. 6; Table 3). Considering the +P+EW treatment, aggregate stability was greatest in the second uppermost layer and lowest in the undermost. Treatments without vegetation did not show any significant modification of the aggregate stability within the depth profile.

3.5. X-ray CT

3.5.1. Soil layer analysis

Soil macroporosity and total segment length of macropores were significantly affected by “depth” (p-values < 0.05). Both variables were largest in the two first uppermost layers and lowest in the two undermost layers Furthermore, total segment lengths in the two uppermost layers were similar as were those in the 3rd and 4th layer, and porosity was maximum in the second uppermost layer (Fig. 7). By contrast, the treatments did not explain the variability of the two response variables at all. However, interaction terms between “treatment” and “depth” were significant (p-values < 0.05) (Table 3). In the +P+EW treatment, total segment length was highest in the second

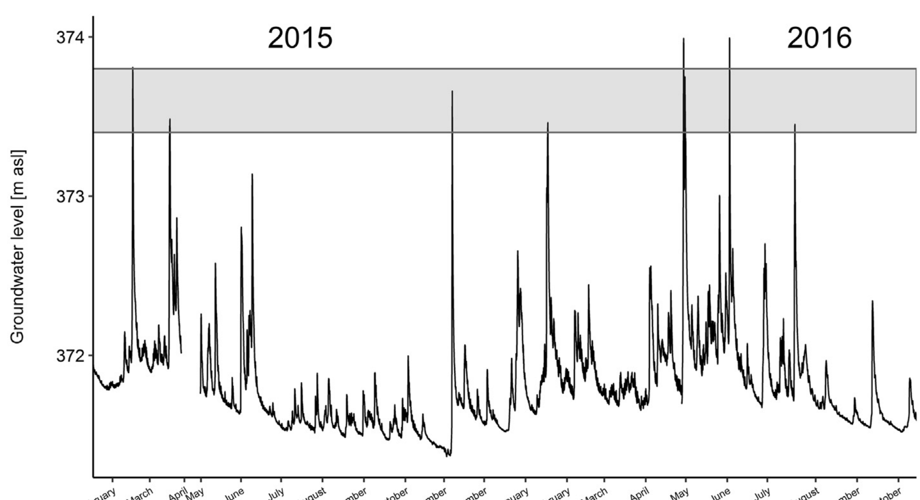

Fig. 3. Groundwater level at the site monitored by a piezometer in the period between February 2015 and October 2016 in close proximity to the plots. The grey rectangle comprises the altitude of the plots above sea level.

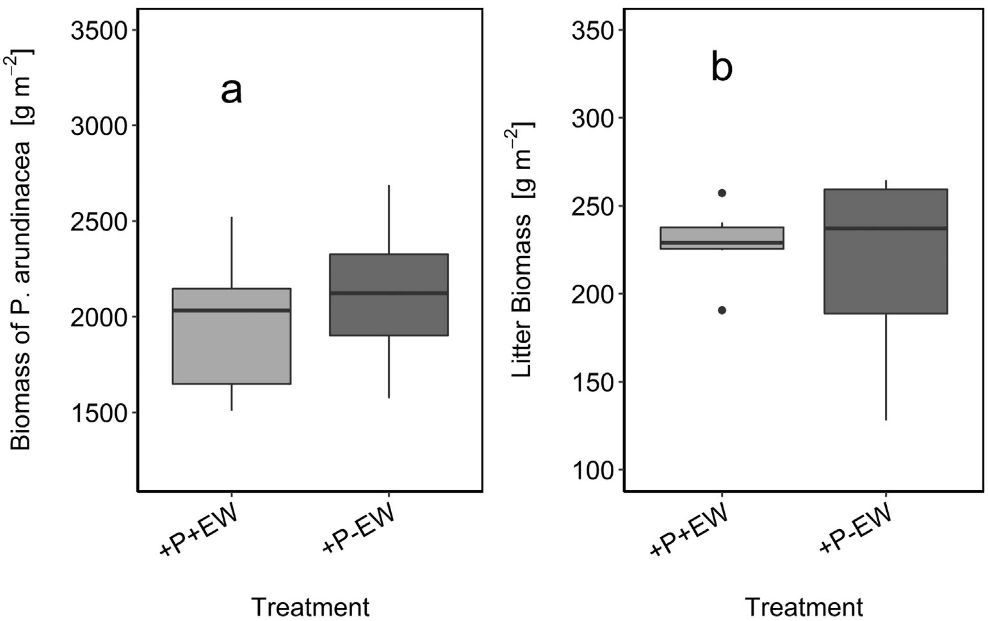

Fig. 4. Vegetation biomass (a) and litter biomass (b) determined after the exposure period of 19 months. P stands for *P. arundinacea* and EW for earthworms.

Table 2
Abundance and biomass of earthworms ± SE collected in October 2016. P stands for *P. arundinacea* and EW for earthworms. Letters a and b represent results from Tukey's HSD tests for one-way ANOVA between the treatments at an α = 0.05 significance level accepting the risk at a p-value < 0.05.

Ecological category	Treatment			
	+P−EW	−P+EW	+P+EW	−P−EW
Earthworm abundance ± SE (individuals plot^{-1})				
Juveniles				
Epigeic	0 ± 0^{a}	0 ± 0^{a}	0 ± 0^{a}	0 ± 0
Endogeic	0 ± 0^{a}	1 ± 1^{a}	2 ± 1^{a}	0 ± 0^{a}
Anecic	$0 \pm 0^{a,b}$	$0 \pm 0^{a,b}$	1 ± 1^{a}	0 ± 0^{b}
Unidentified	7 ± 2^{a}	5 ± 2^{a}	14 ± 4^{a}	6 ± 2^{a}
Total	$7 \pm 2^{a,b}$	6 ± 2^{b}	17 ± 5^{a}	6 ± 2^{b}
Adults				
Epigeic	0 ± 0^{a}	1 ± 1^{a}	0 ± 0^{a}	0 ± 0^{a}
Endogeic	$1 \pm 0^{a,b}$	0 ± 0^{a}	2 ± 1^{b}	$0 \pm 0^{a,b}$
Anecic	1 ± 0^{a}	0 ± 0^{a}	1 ± 0^{a}	1 ± 0^{a}
Unidentified	1 ± 1^{a}	0 ± 0^{a}	1 ± 0^{a}	1 ± 0^{a}
Total	3 ± 1^{a}	1 ± 1^{a}	4 ± 1^{a}	2 ± 1^{a}
Juveniles + adults				
Epigeic	0 ± 0^{a}	1 ± 1^{a}	0 ± 0^{a}	0 ± 0^{a}
Endogeic	1 ± 0^{a}	1 ± 1^{a}	4 ± 2^{a}	0 ± 0^{a}
Anecic	1 ± 1^{a}	0 ± 0^{a}	2 ± 1^{a}	1 ± 0^{a}
Unidentified	8 ± 2^{a}	5 ± 2^{a}	15 ± 5^{a}	7 ± 2^{a}
Total	$10 \pm 3^{a,b}$	7 ± 3^{b}	21 ± 5^{a}	8 ± 3^{b}
Earthworm biomass ± SE (g plot^{-1})				
Juveniles				
Total	$2.25 \pm 0.64^{a,b}$	$2.02 \pm 0.68^{a,b}$	4.12 ± 1.08^{a}	0.82 ± 0.22^{b}
Adults				
Total	$2.70 \pm 1.10^{a,b}$	0.71 ± 0.50^{a}	3.97 ± 0.79^{b}	$1.27 \pm 0.55^{a,b}$
Juveniles + adults				
Total	$4.96 \pm 1.54^{a,b}$	2.73 ± 0.93^{a}	8.09 ± 1.47^{b}	2.09 ± 0.75^{a}

uppermost layer followed by the uppermost one (Fig. 7). In the +P−EW treatment, total segment length decreased along the depth gradient, whereas porosity was significantly increased in the uppermost und the 3rd layer. For treatments without vegetation neither total segment length nor porosity varied with soil depth (Table 3). In contrast to total segment length and porosity, “treatment” significantly affected pore connectivity (p-value < 0.05), in addition to a highly significant “depth” effect (p-value < 0.001). Furthermore, interaction terms between “treatment” and “depth” were significant (Table 3). The presence of *P. arundinacea* significantly improved the pore connectivity within the four levels of “treatment”. Pore connectivity significantly decreased within the depth profile within the four levels of “depth”. Pore connectivity in the two uppermost layers was higher than below in plots with *P. arundinacea* and in those of the −P+EW treatment (Table 3).

3.5.2. *Analysis of new alluvial sediments*

Sediments deposited during the exposure period were analysed for two events: 1) the flood on 21.11.2015 and 2) the sum of three floods in summer 2016 (Fig. 7), as each individual event did not result in a sufficient sediment accumulation to be detected by X-ray CT image analyses. The pre-existing sediment ranging to the soil surface at the beginning of the experiment was summarised as “initial sediment” for

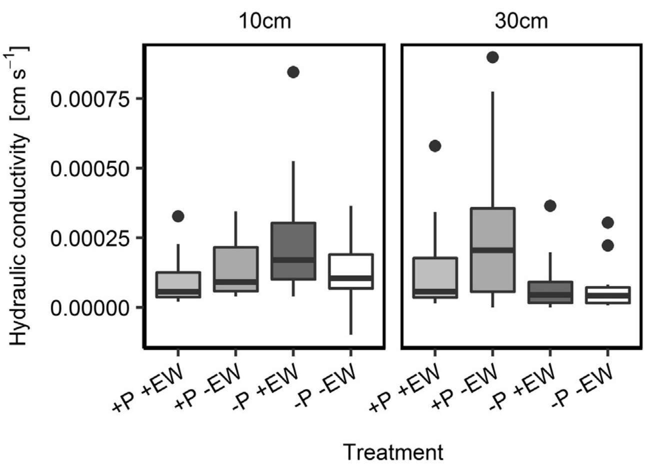

Fig. 5. Boxplots showing the variability of the hydraulic conductivity (Kfs) according to treatments and depths. P denominates *P. arundinacea* and EW earthworms.

the respective plots. Results from the analyses of variance for randomised complete block designs were almost identical for the total segment length and the porosity of the analysed sediments. For both parameters, the factor "treatment" was significant (p-value < 0.05) and the factor "depth" was highly significant (p-value < 0.001) (Table 4). Both total segment length and porosity of the sediments were significantly higher in plots containing *P. arundinacea*. The deposits of 21.11.2015 exhibited both the highest porosity and total segment length, whereas these variables were lowest in the most recent deposit. Also, interaction terms between "treatment" and "depth" were significant (p-value < 0.05). The presence of *P. arundinacea* significantly increased the total segment length and the porosity in the deposit from the 21.11.2015 and in the initial sediment (Table 4). The contribution of "treatment" to explain the variablility of the pore connectivity was highly significant (p-value < 0.001), whereas "depth" and interaction terms did not show any significant contribution (Table 4). However, since the p-value for interaction terms was close to the level of acceptance, multiple comparison tests at the main factor level were nevertheless performed. In summary, pore connectivity was the highest in plots with *P. arundinacea*, whatever the sediment deposition.

4. Discussion

The contribution of *P. arundinacea* and earthworms to soil structure formation in plots installed in a highly dynamic floodplain habitat was successfully analysed by coupling freeze coring and X-ray CT. The results clearly demonstrated the effect of *P. arundinacea* and earthworms in the plots, even though the structural integrity of the freeze cores was not completely warranted (Strasser et al., 2015; Liernur et al., 2017) and plant root galleries and earthworm tunnels could not clearly be distinguished with the resolution provided by the medical scanner.

4.1. Short-term engineering effect of P. arundinacea

P. arundinacea as a pioneer herbaceous plant efficiently structured the two uppermost layers of the initial sediment by improving the pore network, the pore connectivity and the stability of the soil aggregates within 1.5 years. Additionally, these plants were also capable of improving these parameters in the new sediment deposit originating from 21.11.2015. Thus, *P. arundinacea* required only one year, corresponding to one single vegetation period, to improve the soil structure in a recent alluvial deposit. In our study, this efficiency of *P. arundinacea* despite strong impairment by alluvial dynamics was highlighted for the first time. Chantigny et al. (1997) already showed that *P. arundinacea* can significantly contribute to aggregation in agricultural soils in less than three years. In recent micro- and mesocosm experiments, *P. arundinacea* and other pioneer herbaceous plants were able to significantly improve aggregate stability and macro-porous networks of soils and sediments within several weeks (Milleret et al., 2009; Fonte et al., 2012; Kohler-

Table 3
Results for the analyses of variance for randomised split-plot designs. Significant overall and interaction effects were specified by a p-value < 0.05. "n.s." stands for not significant. WSA stands for water stable aggregates, Seglen for segment length, P for *P. arundinacea* and EW for earthworms. Letters a, b, c and d represent results from Tukey's HSD posthoc analysis among the treatments at an $\alpha = 0.05$ significance level accepting the risk at a p-value < 0.05. ":" represents interaction effects between two predictor variables.

Predictor variables and levels	Response variables			
	%WSA	Seglen	Porosity	Pore connectivity
Overall and interaction effects				
Treatment	n.s.	n.s.	n.s.	p < 0.05
Depth	p < 0.001	p < 0.05	p < 0.05	p < 0.001
Treatment:depth	n.s.	p < 0.05	p < 0.05	p < 0.05
Multiple comparisons of "treatments"				
+P−EW	a	a	a	a
−P+EW	a	a	a	b
+P+EW	a	a	a	ab
−P−EW	a	a	a	b
Multiple comparisons of "depth"				
0.0–7.5 cm	a	a	ab	a
7.5–22.5 cm	a	a	a	a
22.5–37.5 cm	ab	b	bc	b
37.5–52.5 cm	b	b	c	c
Multiple comparisons of "treatments" within "depth" levels				
0.0–7.5 cm				
+P−EW	a	a	a	a
−P+EW	b	b	b	b
+P+EW	ab	a	a	a
−P−EW	b	b	b	b
7.5–22.5 cm				
+P−EW	a	ab	a	a
−P+EW	a	b	b	bc
+P+EW	a	a	ab	ab
−P−EW	a	b	b	c
22.5–37.5 cm				
+P−EW	a	a	a	a
−P + EW	a	a	a	a
+P + EW	a	a	a	a
−P−EW	a	a	a	a
37.5–52.5 cm				
+P−EW	a	a	a	a
−P + EW	a	a	a	a
+P+EW	a	a	a	a
−P−EW	a	a	a	a
Multiple comparisons of "depth" within "treatment" levels				
+P−EW				
0.0–7.5 cm	a	a	a	a
7.5–22.5 cm	ab	ab	b	a
22.5–37.5 cm	ab	b	a	b
37.5–52.5 cm	b	c	b	b
−P+EW				
0.0–7.5 cm	a	a	a	a
7.5–22.5 cm	a	a	a	a
22.5–37.5 cm	a	a	a	ab
37.5–52.5 cm	a	a	a	b
+P+EW				
0.0–7.5 cm	ab	ab	a	a
7.5–22.5 cm	a	a	a	a
22.5–37.5 cm	ab	b	a	b
37.5–52.5 cm	b	b	a	b
−P−EW				
0.0–7.5 cm	a	a	a	a
7.5–22.5 cm	a	a	a	a
22.5–37.5 cm	a	a	a	a
37.5–52.5 cm	a	a	a	a

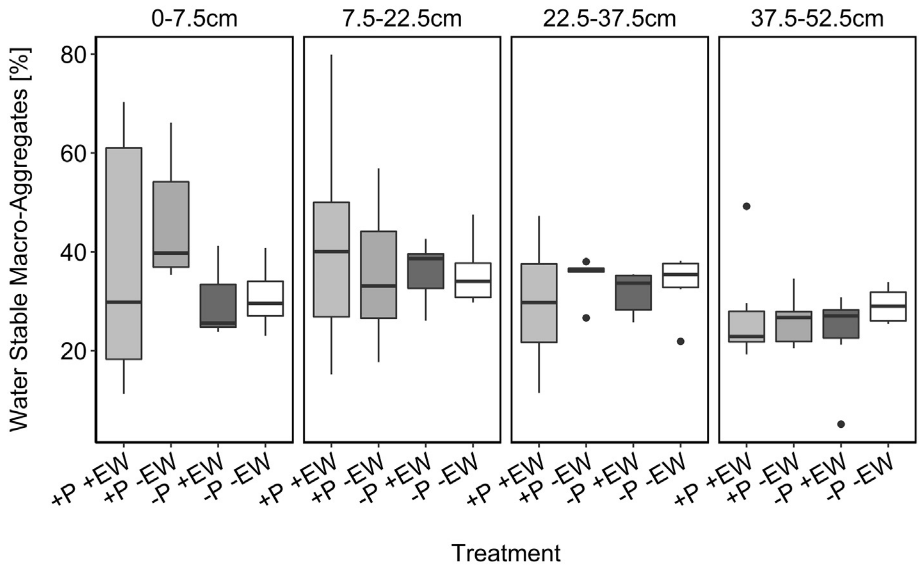

Fig. 6. Boxplots showing the aggregate stability according to the treatments and the depths. P stands for *P. arundinacea* and EW for earthworms.

Milleret et al., 2013). However, the physical conditions, e.g. the temperature and soil moisture contents during the latter experiments were stable and herbaceaous plants were not exposed to waterlogged conditions or to drought and were not exposed to sediment deposition. Both stress factors can damage plant seedlings and inhibit the progress of soil structure formation in close proximity to rivers (Bätz et al., 2015). Therefore, it is even more unexpected that the progress in soil structure formation became clearly visible after one year only. In contrast, the most recent deposits from summer 2016 and the two undermost layers of the initial sediments were not significantly structured by *P. arundinacea*. Most likely, six months were not sufficient to structure a fresh alluvial deposit.

4.2. Short-term engineering effect of earthworms

In contrast to *P. arundinacea*, earthworms contributed to soil structure formation only to a small extent within 1.5 years. In presence of earthworms, pore connectivity was positively affected in the two uppermost layers and the aggregate stability showed a slight increase in the second uppermost layer. The second uppermost layer corresponded to the zone preferentially resided by endogeic and anecic earthworms. In general, earthworms are known to be highly efficient soil engineers that significantly improve the structural stability of soils (Brown et al., 2000; Six et al., 2002). However, environmental conditions at the Thur River were most likely less favourable for earthworms, e.g. large proportions of sand, low organic matter contents and high water level fluctuations in the soil can result in a low total abundance and thus to their engineering capacity. Total abundance was up to 10 times lower compared to other floodplain habitats in Switzerland which were sampled with the same method (Bullinger-Weber et al., 2007, 2012; Salomé et al., 2011; Fournier et al., 2012). On one hand, the textural composition of the sediments was most likely problematic for earthworms. Large proportions of coarse sand (around 80% in this case) lead to skin and intestinal damages of earthworms during burrowing activity, most likely explaining the low presence of endogeics and anecics (Edwards and Bohlen, 1996; Curry and Schmidt, 2007). Results of a recent study indicate that the endogeic speices *A. chlorotica* preferentially chose the finer textured alluvial sediment, when sediments of different textural composition are superimposed. On the other hand, numerous studies report that the abundance of earthworms is crucially reduced in presence of strong alluvial dynamics (Ausden et al., 2001; Plum and Filser, 2005; Ivask et al., 2007). Nevertheless, earthworms have developed physiological and morphological adaptations to survive water-saturated conditions for a certain time (Plum and Filser, 2005; Zorn et al., 2008) or produce water-resistant cocoons (Roots, 1956; Plum and Filser, 2005). Most likely, larger communities of earthworms could not be developed as a consequence of the high proportion of sand.

4.3. Interactions between P. arundinacea and earthworms

The abundance of earthworms was increased by factor 2.5 in presence of *P. arundinacea*. Conversely, biomass of *P. arundinacea* was not affected by the presence of earthworms. Earthworms could benefit from the shadowing effect of the vegetation which generally moderates the soil temperature and retards the desiccation of the soil in dry periods. Habitats in close proximity to rivers, which are mostly sparsely covered by vegetation, are often subject to severe summer droughts (Naiman et al., 2000; Nilsson and Berggren, 2000; Bätz et al., 2014). On the other hand, plants provide OM inputs through above-ground litter biomass and through root exudates belowground which can be beneficial for earthworms (Yavitt et al., 2015). These inputs are especially important in coarse textured soils or under nutrient poor soil conditions (Laossi et al., 2010; Blouin et al., 2013). However, the contribution of earthworms to soil structure formation in the vegetation treatments was difficult to assess, as the single effects of *P. arundinacea* massively exceeded the effects of earthworms. As a consequence, neither aggregate stability measurements nor X-ray analyses revealed any interaction effects between *P. arundinacea* and earthworms. Generally, findings of recent meso- and microcosm studies strongly suggest that several plant and earthworm species can contribute concomitantly to soil structure formation (Zangerlé et al., 2011; Fonte et al., 2012; Kohler-Milleret et al., 2013). Several plants use earthworm tunnels for root network extension and preferentially colonise their nutrient enriched casts and burrow walls (Spiers et al., 1986; Zaller and Arnone, 1999, Decaëns et al., 2011). Earthworms take advantage of easy decomposable OM released by plant roots as an energy source or feed directly on small dead plant roots (Gilbert et al., 2014; Sanchez-de Leon et al., 2014; Yavitt et al., 2015).

4.4. Effects of P. arundinacea and earthworms on the field saturated hydraulic conductivity

Values for field saturated hydraulic conductivity were comparable to those from other studies measured in sandy soils (Rodgers and Mulqueen, 2004; Lewis, 2016; Rezaei et al., 2016). This soil property was not modified by the treatments despite extension of the macro-

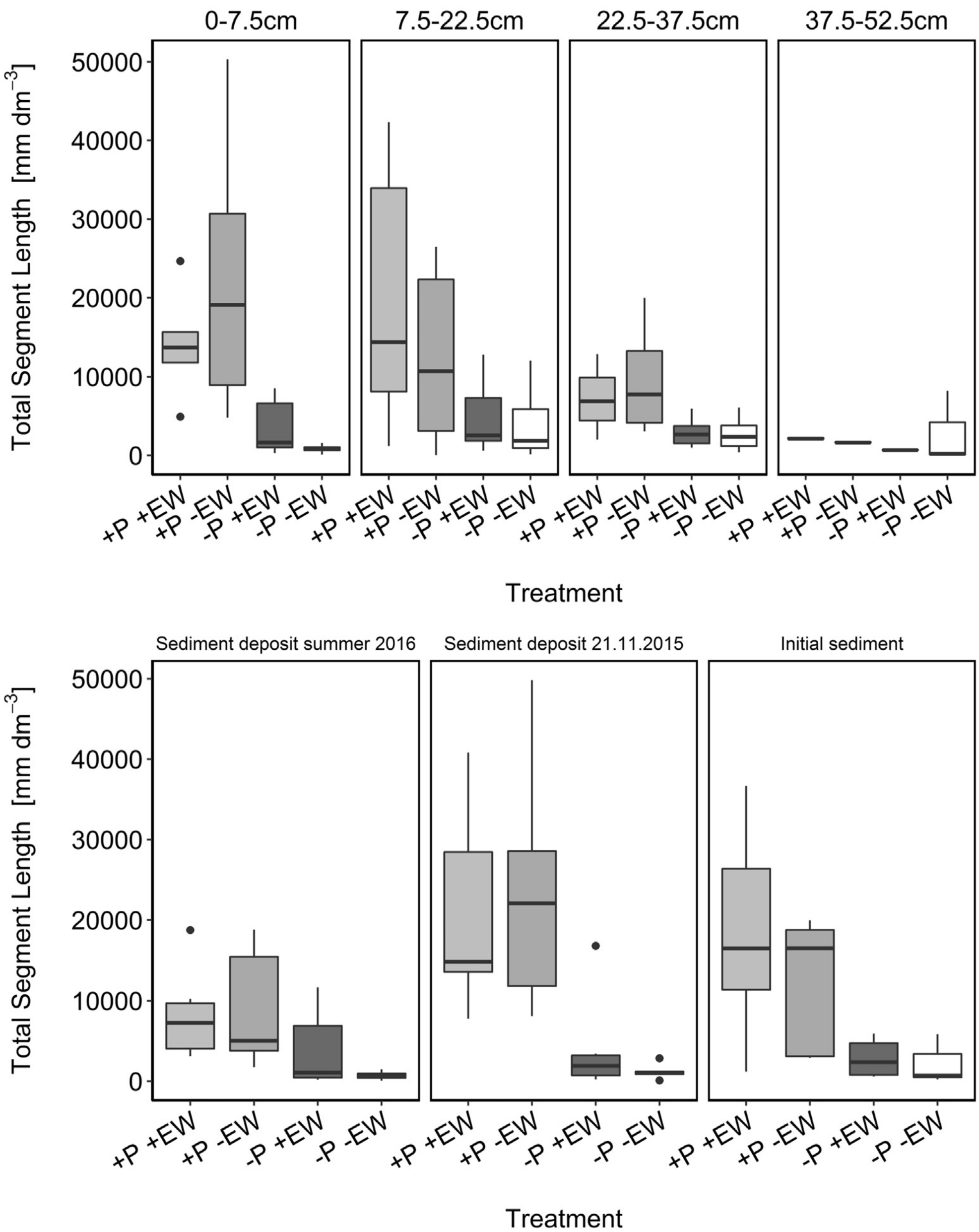

Fig. 7. Boxplots showing the total segment length according to the treatments and the depths. P stands for *P. arundinacea* and EW for earthworms.

porous network, especially in plots containing *P. arundinacea*. Generally, hydraulic conductivity is a parameter which can vary over orders of magnitude across short distances. Hydraulic properties can be significantly improved in the presence of plants and earthworms, leading to an increased water infiltration rate (Gurnell and Petts, 2006; Jouquet et al., 2011; Guéi et al., 2012). This can result in a decrease of soil erosion by > 50% during precipitation events, as surface water runoff is strongly reduced (Shuster et al., 2002; Shipitalo et al., 2004). In the plots at the Thur River, hydraulic properties were potentially altered by alluvial dynamics in the plots. Flood events can restructure the pore system and clog macro-pores through the deposition of fine sediment particles (Bottinelli et al., 2010; Gianni et al., 2016). Furthermore, the textural composition of the sediments in dynamic floodplain habitats strongly varies in space and time.

4.5. Future challenges for management strategies of near natural and restored floodplains

In the course of current river restoration projects in Switzerland, simple and efficient solutions are sought to stabilise the river shore. Our results indicate that *P. arundinacea* is a highly efficient soil engineer in areas which are strongly threatened by alluvial dynamics. Furthermore, *P. arundinacea* contributed immediately to soil structure formation and significantly increased the macro-porous system and the structural stability of aggregates after only one year. However, the frequency and magnitude of flood events at the Thur River in 2015 and 2016 were lower compared to the years before. In the recent past, a larger amount of intermediate and strong flood caused stronger erosion and the deposition of large sediment layers in the Thur River floodplain (Schirmer et al., 2014; Schomburg et al., 2018). One single event can bury seedlings of herbaceous plants and interrupt the progress of soil structure formation. Furthermore, fluctuating groundwater levels can also strongly affect the vegetation leading to conditions in the rhizosphere

Table 4
Results for the analyses of variance for randomised split-plot designs for recent alluvial deposits. Significant overall and interaction effects were specified by a p-value < 0.05. "n.s." stands for not significant. WSA stands for water stable aggregates, Seglen for segment length, P for *P. arundinacea* and EW for earthworms. Letters a and b represent results from Tukey's HSD posthoc analysis for the treatments at an $\alpha = 0.05$ significance level accepting the risk at a p-value < 0.05. ":" represents interaction effects between two predictor variables.

Predictor variables and levels	Response variables		
	Seglen	Porosity	Pore connectivity
Overall and interaction effects			
Treatment	p < 0.05	p < 0.05	p < 0.001
Depth	p < 0.001	p < 0.001	n.s.
Treatment:depth	p < 0.05	p < 0.05	n.s.
Multiple comparisons of "treatments"			
+ P − EW	a	a	a
− P + EW	b	b	b
+ P + EW	a	a	a
− P − EW	b	b	b
Multiple comparisons of "depth"			
Sediment deposit summer 2016	b	b	a
Sediment deposit 21.11.2015	a	a	a
Initial sediment	ab	ab	a
Multiple comparisons of "treatments" within "depth" levels			
Sediment deposit summer 2016			
+ P − EW	a	a	a
− P + EW	a	a	b
+ P + EW	a	a	a
− P − EW	a	a	b
Sediment deposit 21.11.2015			
+ P − EW	a	a	a
− P + EW	b	b	b
+ P + EW	a	a	a
− P − EW	b	b	b
Initial sediment			
+ P − EW	ab	a	a
− P + EW	b	b	b
+ P + EW	a	a	a
− P − EW	b	b	b
Multiple comparisons of "depth" within "treatment" levels			
+ P − EW			
Sediment deposit summer 2016	b	b	a
Sediment deposit 21.11.2015	a	a	a
Initial sediment	b	a	a
− P + EW			
Sediment deposit summer 2016	a	a	a
Sediment deposit 21.11.2015	a	a	a
Initial sediment	a	a	a
+ P + EW			
Sediment deposit summer 2016	b	b	a
Sediment deposit 21.11.2015	a	a	a
Initial sediment	a	ab	a
− P − EW			
Sediment deposit summer 2016	a	a	a
Sediment deposit 21.11.2015	a	a	a
Initial sediment	a	a	a

alternating between water saturation and drought. In 2015 and 2016 which were marked by hot and dry summer periods, the plots were only saturated three times by rising groundwater levels without surface water entering the floodplain. Nevertheless, Schomburg et al. (2018) clearly demonstrated that fluctuating groundwater levels strongly control the development of plant communities and thus their capability to contribute significantly to soil structure formation. On one hand, the herbaceous vegetation community is strongly affected by alluvial dynamics. On the other hand, it can rapidly recover in case of destruction, by means of viable seeds that are transported and deposited at the river shore during flood events (Gurnell, 2007; Corenblit et al., 2009). However, not only seeds of native herbaceous plants are deposited, but also non-native species being able to become invasive. Some of the invasive species can even have negative effects on the soil structure in floodplain habitats. The Himalayan *Impatiens glandulifera*, which was also found at the Thur River can outcompete native species (Chapman and Gray, 2012) and is able to trap sediments with their shallow root system. However, increased soil erosion rates were recorded in habitats settled by *I. glandulifera* as the plants die in late autumn due to their intolerance towards cold temperatures (Greenwood et al., 2018). The bare soil is thus unprotected towards floods in the winter season (Skálová et al., 2011).

5. Conclusions

This study investigated the effect of the herbaceous pioneer plant species *P. arundinacea* and earthworms on soil structure formation under consideration of strong alluvial dynamics in a restored floodplain section within a period of 19 months. The coupling of freeze coring and X-ray CT provided clear results about the recent development of a soil structure in controlled field plots. The article highlights the novelty that *P. arundinacea* can significantly improve soil structure of recent alluvial sediments within only one year. Earthworms alone did not improve the soil structure within the exposure period, most likely due to the large proportion of sand in the deposits. They however promoted the effect of soil structure formation in presence of *P. arundinacea*. Reciprocally, *P. arundinacea* increased the total abundance of earthworms. Thus, our results strongly suggest that herbaceous plants, such as *P. arundinacea*, can play a key role for the initial soil structure formation in near-natural and restored floodplains in the short-term. The colonisation of river shores by pioneer herbaceous plants and earthworms thus should be promoted to improve the success of river restoration projects.

Acknowledgements

The present study was developed in the framework of the FloodSTRESS project funded by the Swiss National Science Foundation (SNF), project no. FN 315230_153460, the CCES-project RECORD Catchment of the ETH domain and internal funds of the Swiss Federal Research Institute WSL. M. Riaz acknowledges the funding by a Swiss Government Excellence Scholarship and an International Short Visit Grant from SNF (project no. IZK0Z2_170958). The authors gratefully thank the following institutions and people for their highly valuable support in the field and in the lab: the University Center for Legal Medicine Lausanne – Geneva (CURML), especially Kewin Ducrot, the FiBL institute in Frick, especially Anton Kuhn and Simon Tresch, the UWITEC company, Vincent Gruber, Filip Kristic and Florian Migliarini, Dr. Pascal A. Niklaus, the workshop of WSL Davos, Roger Köchli, Anaïs Cattin, Elio Wildisen and Marcel Müller (all WSL).

Appendix A. Formula for the calculation of the field saturated hydraulic conductivity from the infiltration test performed using the Guelph Permeameter

$$K_{fs} = G_2 Q_2 - G_1 Q_1 \tag{1}$$

$$G_1 = \frac{H_2 C_1}{\pi(2H_1 H_2 (H_2 - H_1) + a^2 (H_1 C_2 - H_2 C_1))} \tag{2}$$

$$G_2 = \frac{H_1 C_2}{\pi(2H_1H_2(H_2 - H_1) + a^2(H_1C_2 - H_2C_1))} \quad (3)$$

$$Q_1 = YR_1 \quad (4)$$

$$Q_2 = YR_2 \quad (5)$$

Y representing the inner reservoir constant of 2.16, *R1* and *R2* the steady state fall rates of water in the reservoir at head height *H1* and *H2*, respectively, and *a* the radius of the well. Equations for shape factors *C1* and *C2* depend on the soil texture-structure category which were adapted according to Elrick et al. (1989) and Zhang et al. (1998). Decisions for the shape factor equations were made based on the soil texture analyses of the sediments.

$$K_{fs} = \frac{C_1 Q_1}{2\pi H_1^2 + \pi a^2 C_1 + 2\pi\left(\frac{H_1}{\alpha^*}\right)} \quad (6)$$

Here α^* represents the macroscopic capillarity length parameter that also depends on the soil texture-structure category. Values are provided by Elrick et al. (1989).

Appendix B. Example of an image slice projected in Avizo. Grey-shades represent the soil matrix and organic matter, black colours the void corresponding to pores (a). The blue colour represents the void after binarisation (b) that represents the porosity calculated relative to the soil matrix using the material statistics function provided in Avizo

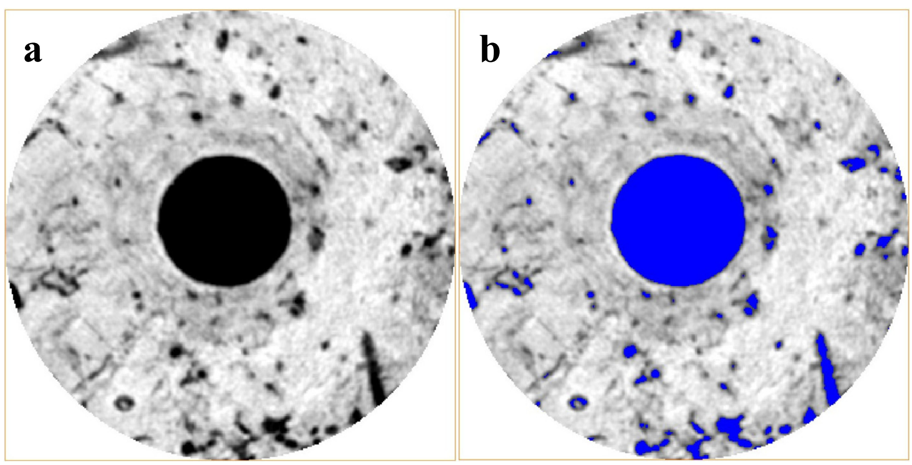

References

Acreman, M.C., Riddington, R., Booker, D.J., 2003. Hydrological impacts of floodplain restoration: a case study of the River Cherwell, UK. Hydrol. Earth Syst. Sci. 7, 75–85.
Amossé, J., Turberg, P., Kohler-Milleret, R., Gobat, J.-M., Le Bayon, R.-C., 2015. Effects of endogeic earthworms on the soil organic matter dynamics and the soil structure in urban and alluvial soil materials. Geoderma 243–244, 50–57.
Angers, D.A., Caron, J., 1998. Plant-induced changes in soil structure: processes and feedbacks. Biogeochemistry 42, 55–72.
Arnhold, E., 2013. Package in the R environment for analysis of variance and complementary analyses. Braz. J. Vet. Res. Anim. Sci. 50 (6).
Auguie, B., 2016. gridExtra: miscellaneous functions for "grid" graphics. https://CRAN.R-project.org/package=gridExtra.
Ausden, M., Sutherland, W.J., James, R., 2001. The effects of flooding lowland wet grassland on soil macroinvertebrate prey of breeding wading birds. J. Appl. Ecol. 38, 320–338.
Bätz, N., Verrecchia, E., Lane, S.N., 2014. Soil in braided rivers: an overlooked component of braided river morphodynamics. In: Schleiss (Ed.), 2014: River Flow. Tylor & Francis Group, London.
Bätz, N., Verrecchia, E.P., Lane, S.N., 2015. Organic matter processing and soil evolution in a braided river system. Catena 126, 86–97.
Blakemore, R.J., 2008. An Updated List of Valid, Invalid and Synonym Names of Criodrioidea (Criodrilidae) and Lumbricoidea (Annelida: Oligochaeta: Sparganophilidae, Ailoscolecidae, Hormogastridae, Lumbricidae, and Lutodrilidae). Yokohama National University.
Blanchart, E., Lavelle, P., Braudeau, E., Le Bissonais, Y., Valentin, C., 1997. Regulation of soil structure by geophagous earthworm activites in humid savannas of Côte d'Ivoire. Soil Biol. Biochem. 29, 431–439.
Blouin, M., Hodson, M.E., Delgado, E.A., Baker, G., Brussaard, L., Butt, K.,.R., Dai, J., Dendooven, L., Peres, G., Tondoh, J.E., Cluzeau, D., Brun, J.-J., 2013. A review of earthworm impact on soil function and ecosystem services. Eur. J. Soil Sci. 64, 161–182.
Bottinelli, N., Henry-de-Tureaux, T., Hallaire, V., Mathieu, J., Benard, Y., Duc Tran, T., Jouquet, P., 2010. Earthwoms accelerate soil porosity turnover under watering conditions. Geoderma 156, 43–47.
Bouché, M., 1972. Lombriciens de France. Ecologie et systématique INRA Publ. Institut National des Recherches Agriculturelles, Paris.
Brown, G.G., Barois, I., Lavelle, P., 2000. Regulation of soil organic matter dynamics and microbial activity in the drilosphere and the role of interactions with other edaphic functional domains. Eur. J. Soil Biol. 36, 177–198.
Brussard, L., Kooistra, M.J., 1993. Soil Structure/Soil Biota Interrelationsships. Elsevier Science, Amsterdam.
Bullinger-Weber, G., Le Bayon, R.-C., Guenat, C., Gobat, J.-M., 2007. Influence of some physicochemical and biological parameters in soil structure formation in alluvial soils. Eur. J. Soil Biol. 43, 57–70.
Bullinger-Weber, G., Guenat, C., Gobat, J.-M., Le Bayon, R.-C., 2012. Impact of flood deposits on earthworm communities in alder forests from a subalpine floodplain (Kandersteg, Switzerland). Eur. J. Soil Biol. 49, 5–11.
Bundesamt für Umwelt BAFU, 2008. Auendossier: Faktenblätter. Vollzug Umwelt VU, Ittingen.
Bundesamt für Umwelt BAFU, 2015. Renaturierung der Schweizer Gewässer. Die Sanierungspläne der Kantone ab 2015. Ittingen, vol. 16.11.2015.
Bundesamt für Umwelt BAFU, 2017. Vollzugshilfe Renaturierung der Gewässer. Ittingen.
Capowiez, I., Sammartino, S., Michel, E., 2011. Using X-ray tomography to quantify earthworm bioturbation non-destructively in repacked soil cores. Geoderma 162, 124–131.
Capowiez, I., Bottinelli, N., Sammartino, S., Jouquet, P., 2015. Morphological and functional characterisation of the burrow systems of six earthworm species (Lumbricidae). Biol. Fertil. Soils 51, 869–877.
Chantigny, M.H., Angers, D.A., Prévost, D., Vézina, L.-P., Chalifour, F.-P., 1997. Soil aggregation and fungal and bacterial biomass under annual and perennial cropping systems. Soil Sci. Soc. Am. J. 61, 262–267.
Chapman, D.S., Gray, A., 2012. Complex interactions between the wind and ballistic seed dispersal in Impatiens glandulifera (Royle). J. Ecol. 100, 874–883.
Corenblit, D., Steiger, J., Gurnell, A.M., Tabacchi, E., Roques, L., 2009. Control of

sediment dynamics by vegetation as a key function driving biogeomorphic succession within fluvial corridors. Earth Surf. Process. Landf. 34, 1790–1810.
Crouzy, B., Perona, P., 2012. Biomass selection by floods and related timescales. Part 2: stochastic modeling. Adv. Water Resour. 39, 97–105.
Curry, J.P., Schmidt, O., 2007. The feeding ecology of earthworms: a review. Pedobiologia 50, 463–477.
Czarnes, S., Hallett, P.D., Bengough, A.G., Young, I.M., 2000. Root- and microbial-derived mucilages affect soil structure and water transport. Eur. J. Soil Sci. 51, 435–443.
Dalal, R.C., Bridge, B.J., 1996. Aggregation and organic matter storage in sub-humid and semi-arid soils. In: Carter, M.R., Stewart, B.A. (Eds.), Structure and Organic Matter Storage in Agricultural Soils. CRC Press, Boca Raton, FL, pp. 263–307.
Decaëns, T., Margerie, P., Renault, J., Bureau, F., Aubert, M., Hedde, M., 2011. Niche overlap and species assemblage dynamics in an aging pasture gradient in north-western France. Acta Oecol. 37, 212–219.
Degens, B.P., Sparling, G.P., Abbott, L.K., 1994. The contribution from hyphae, roots and organic carbon constituents to the aggregation of a sandy loam under long-term clover-based and grass pastures. Eur. J. Soil Sci. 45, 459–468.
Diaz-Zorita, M., Perfect, E., Grove, J., 2002. Disruptive methods for assessing soil structure. Soil Tillage Res. 64, 3–22.
Edwards, C.A., Bohlen, P.J., 1996. Biology and Ecology of Earthworms, Band 3. (Springer Science & Business Media).
Ehlers, W., 1975. Observations on earthworm channels and infiltration on tilled and untilled loess soil. Soil Sci. 119, 242–249.
Elrick, D.E., Reynolds, W.D., Tan, K.A., 1989. Hydraulic conductivity measurements in the unsaturated zone using improved well analyses. Ground Water Monit. Rev. 9, 184–193.
FEI, 2016. Amira & Avizo 3D software. [WWW Document]. URL. https://www.fei.com/software/amira-avizo/, Accessed date: 4 April 2018.
Fonte, S.J., Quintero, D.C., Velasquez, E., Lavelle, P., 2012. Interactive effects of plants and earthworms on the physical stabilization of soil organic matter in aggregates. Plant Soil 359, 205–214.
Fournier, B., Samaritani, E., Shrestha, E., Mitchell, E.A.D., Le Bayon, R.-C., 2012. Community ecology of earthworm in a restored floodplain and potential as bioindicators of river restoration. Appl. Soil Ecol. 59, 87–95.
Fournier, B., Guenat, C., Bullinger-Weber, G., Mitchell, E.A.D., 2013. Spatio-temporal heterogeneity of riparian soil morphology in a restored floodplain. Hydrol. Earth Syst. Sci. 17, 4031–4042.
Franchini, A.G., Zeyer, J., 2012. Freeze-coring method for characterization of microbial community structure and function in wetland soils at high spatial resolution. Appl. Environ. Microbiol. 78, 4501–4504.
Gee, G.W., Bauder, J.W., 1986. Particle size analysis. In: Klute (Ed.), Methods of Soil Analysis, Part A, 2nd edition. vol. 9. American Society of Agronomy, Madison, WI, pp. 383–411 (n.d.).
Gianni, G., Richon, J., Perrochet, P., Vogel, A., Brunner, P., 2016. Rapid identification of transience in streambed conductance by inversion of floodwave responses. Water Resour. Res. 52, 2647–2658.
Gilbert, K.J., Fahey, T.J., Maerz, J.C., Sherman, R.E., Bohlen, P., Dombroskie, J.J., Groffman, P.M., Yavitt, J.B., 2014. Exploring carbon flow through the root channel in a temperate forest soil food web. Soil Biol. Biochem. 76, 45–52.
Graf-Rosenfellner, M., Cierjacks, A., Kleinschmit, B., Lang, F., 2016. Soil formation and its implications for stabilization of soil organic matter in the riparian zone. Catena 139, 9–18.
Greenwood, P., Walling, D.E., Quine, T.A., 2013. Using caesium-134 and cobalt-60 as tracers to assess the remobilization of recently-deposited overbank-derived sediment on river floodplains during subsequent inundation events. Earth Surf. Process. Landf. 39 (2), 228–244.
Greenwood, P., Baumann, P., Pulley, S., Kuhn, N.J., 2018. The invasive alien plant *Impatiens glandulifera* (Himalayan Balsam), and increased soil erosion: causation or association? Case studies from a river system in Switzerland and the UK. J. Soils Sediments 18, 3463–3477.
Guéi, A.M., Baidai, Y., Tondoh, J.E., Huising, J., 2012. Functional attributes: compacting vs decompacting earthworms and influence on soil structure. Curr. Zool. 58, 556–565.
Guenat, C., Bureau, F., Weber, G., Toutain, F., 1999. Initial stages of soil formation in a riparian zone: importance of biological agents and lithogenic inheritance in the development of the soil structure. Eur. J. Soil Biol. 35, 153–161.
Gurnell, A., 2007. Analogies between mineral sediment and vegetative particle dynamics in fluvial systems. Geomorphology 89, 9–22.
Gurnell, A., 2014. Plants as river system engineers. Earth Surf. Process. Landf. 39, 4–25.
Gurnell, A., Petts, G., 2002. Island-dominated landscapes of large floodplain rivers, a European perspective. Freshw. Biol. 47, 581–600.
Gurnell, A., Petts, G., 2006. Trees as riparian engineers: the Tagliamento River, Italy. Earth Surf. Process. Landf. 31, 1558–1575.
Hayashi, H., Shimatani, Y., Shigematsu, K., Nishihiro, J., Ikematsu, S., Kawaguchi, Y., 2011. A study of seed dispersal by flood flow in an artificially restored floodplain. Landsc. Ecol. Eng. 8, 129–143.
Humpesch, U.H., Niederreiter, R., 1993. Freeze-core method for sampling the vertical distribution of the macrozoobenthos in the main channel of a large deep river, the River Danube at river kilometre 1889. River Systems 9, 87–90.
Iassonov, P., Gebrenegus, T., Tuller, M., 2009. Segmentation of X-ray computed tomography images of porous materials: a crucial step for characterization and quantitative analysis of pore structures. Water Resour. Res. 45, 1–12.
IUSS Working Group WRB, 2006. Guidelines for soil description. FAO, Rome.
Ivask, M., Truu, J., Kuu, A., Truu, M., Leito, A., 2007. Earthworm communities of flooded grasslands in Matsalu, Estonia. Eur. J. Soil Biol. 43, 71–76.
Jouquet, P., Phuong, N.T., Hanh, N.H., Henry-des-Tureaux, T., Chevallier, T., Toan, T.D., 2011. Laboratory investigation of organic matter mineralization and nutrient leaching from earthworm casts produced by Amynthas khami. Appl. Soil Ecol. 47, 24–30.
Junk, W.J., Welcomme, R.L., 1990. Floodplains. Wetlands and Shallow Continental Water Bodies. vol. 1. pp. 491–524.
Kemper, W. D., Rosenau, R. C., 1986. Aggregate stability and size distribution. Pages 425–442 in K. ed. American Society of Agronomy - Soil Science Society of America, editor. Methods of soil analysis, Part 1. Agronomy Monograph no 9. ASA and SSSA, Madison, WI.
Kohler-Milleret, R., Le Bayon, R.-C., Chenu, C., Gobat, J.-M., Boivin, P., 2013. Impact of two root systems, earthworms and mycorrhizae on the physical properties of an unstable silt loam Luvisol and plant production. Plant Soil 370, 251–265.
Kong, A.Y.Y., Six, J., 2010. Tracing roots vs. residue carbon into soils from conventional and alternative cropping systems. Soil Sci. Soc. Am. J. 74, 1201–1210.
Laossi, K.-R., Decaëns, T., Jouquet, P., Barot, S., 2010. Can we predict how earthworm effects on plant growth vary with soil properties? Appl. Environ. Soil Sci. 1–6 784342 (6 pages).
Lavelle, P., Spain, A., 2001. Soil Ecology. Springer, Netherlands. https://doi.org/10.1007/0-306-48162-6.
Lavelle, P., Bignell, D., Lepage, M., Wolters, V., Roger, P., Ineson, P., Heal, O.W., Dhillion, S., 1997. Soil function in a changing world: the role of invertebrate ecosystem engineers. Eur. J. Soil Biol. 33, 159–193.
Lawrence, A.P., Bowers, M.A., 2002. A test of the hot mustard extraction method of sampling earthworms. Soil Biol. Biochem. 34, 549–552.
Le Bayon, R.-C., Bullinger-Weber, G., Gobat, J.-M., Guenat, C., 2013. Chapter 3: Earthworm Communities as Indicators for Evaluating Floodplain Restoration Success in Floodplains, Environmental Management, Restoration and Ecological Implications. Environemental Research Advances. Enner Herenio Alcantara, Nova publishers, New York (241 pp.).
Le Bayon, R.C., Bullinger-Weber, G., Schomburg, A., Turberg, P., Schlaepfer, R., Guenat, C., 2017. Earthworms as ecosystem engineers: a review. In: Earthworms: Types, Roles and Research. NOVA Science Publishers, New York, pp. 129–178.
Lewis, J., 2016. A simple field method for assessing near-surface saturated hydraulic conductivity. Groundwater 54 (5), 740–744.
Liernur, A., Schomburg, A., Turberg, P., Guenat, C., Le Bayon, R.-C., Brunner, P., 2017. Coupling X-ray computed tomography and freeze-coring for the analysis of fine-grained low-cohesive soils. Geoderma 308, 171–186.
Lin, H., Bouma, J., Wilding, L.P., Richardson, J.L., Kutilek, M., Nielsen, D.R., 2005. Advances on Hydropedology. Adv. Agron. 85, 1–89.
Lin, H., McDonnell, J.J., Nimmo, J.R., Pachepsky, Y., 2015. Hydropedology: synergistic integration of soil science and hydrology in the critical zone. Hydrol. Process. 29, 4559–4561.
Liu, C., Walling, D.E., He, Y., 2018. Review: the international sediment initiative case studies of sediment problems in river basins and their management. Int. J. Sediment Res. 33 (2), 216–219.
Ma, Y.-J., Li, X.-Y., Guo, L., Lin, H., 2017. Hydropedology: interactions between pedologic and hydrologic processes across spatiotemporal scales. Earth Sci. Rev. 171, 181–195.
Malmqvist, B., Rundle, S., 2002. Threats to the running water ecosystems of the world. Environ. Conserv. 29, 134–153.
Mardhiah, U., Caruso, T., Gurnell, A., Rillig, M.C., 2014. Just a matter of time: fungi and roots significantly and rapidly aggregate soil over four decades along the Tagliamento River, NE Italy. Soil Biol. Biochem. 75, 133.142.
Milleret, R., Le Bayon, R.-C., Gobat, J.M., 2009. Root, mycorrhiza and earthworm interactions: their effects on soil structuring processes, plant and soil nutrient concentration and plant biomass. Plant Soil 316, 1–12.
Murer, E.J., Baumgarten, A., Eder, G., Gerzabek, M.H., Kandeler, E., Rampazzo, N., 1993. An improved sieving machine for estimation of soil aggregate stability (SAS). Geoderma 56, 539–547.
Naiman, R.J., Décamps, H., 1997. The ecology of interfaces: riparian zones. Annu. Rev. Ecol. Syst. 28, 621–658.
Naiman, R.J., Bilby, R.E., Bisson, P.A., 2000. Riparian ecology and management in the pacific coastal rain forest. Bioscience 50, 996–1011.
Nilsson, C., Berggren, K., 2000. Alterations of riparian ecosystems caused by river regulation. Bioscience 50, 783–792.
Otsu, N., 1979. A threshold selection method from gray-level histograms. IEEE Trans. Syst. Man. Cybern. 9, 62–66.
Partington, D., Therrien, R., Simmons, C.T., Brunner, P., 2017. Blueprint for a coupled model of sedimentology, hydrology, and hydrogeology in streambeds. Rev. Geophys. 55, 287–309.
Pérès, G., Cluzeau, D., Curmi, P., Hallaire, V., 1998. Earthworm activity and soil structure changes due to organic enrichments in vineyard systems. Biol. Fertil. Soils 27, 417–424.
Perona, P., Molnar, P., Crouzy, B., Perucca, E., Jiang, Z., MeLelland, S., Wüthrich, D., Edmaier, K., Francis, R., Camporeale, C., Gurnell, A., 2012. Biomass selection by floods and related timescales: part 1. Experimental observations. Adv. Water Resour. 39, 85–96.
Plum, M., Filser, J., 2005. Floods and drought: response of earthworms and potworms (Oligochaeta: Lumbricidae, Enchytraeidae) to hydrological extremes in wet grassland. Pedobiologia 49, 443–453.
R Core Team, 2013. R: A Language and Environment for Statistical Computing. R Foundation for Statistical Computing, Vienna, Austria URL. http://www.R-project.org/.
Reynolds, W.D., Elrick, D.E., 1985. In situ measurement of field-saturated hydraulic conductivity, sorptivity and the α-parameter using the Guelph permeameter. Soil Sci. 140 (4), 292–302.
Reynolds, W.D., Elrick, D.E., Youngs, E.G., Amoozegar, A., Booltink, H.W.G., Bouma, J.,

2002. Saturated and field-saturated water flow parameters. In: Dane, J., Topp, C. (Eds.), Methods of Soil Analysis, Part 4. Physical Methods. SSSA, Madison, WI, pp. 797–878.
Rezaei, M., Seuntjens, P., Shahidi, R., Joris, I., Boënne, W., Al-Barri, B., Cornelis, W., 2016. The relevance of in-situ and laboratory characterization of sandy soil hydraulic properties for soil water simulations. J. Hydrol. 534, 251–265.
Rodgers, M., Mulqueen, J., 2004. Field-saturated hydraulic conductivity of soil from laboratory constant-head well tests. Irrig. Drain. Syst. 18, 315–327.
Roots, B.I., 1956. The water relations of earthworms II: resistance to desiccation and immersion, and behavior when submerged and when allowed a choice of environment. J. Exp. Biol. 33, 29–44.
Salomé, C., Guenat, C., Bullinger-Weber, G., Gobat, J.-M., Le Bayon, R.-C., 2011. Earthworm communities in alluvial forests: influence of altitude, vegetation stages and soil parameters. Pedobiologia 54, 89–98.
Sanchez-de Leon, Y., Lugo-Perez, J., Wise, D.H., Jastrow, J.D., Gonzalez-Meler, M.A., 2014. Aggregate formation and carbon sequestration by earthworms in soil from a temperate forest exposed to elevated atmospheric CO2: a microcosm experiment. Soil Biol. Biochem. 68, 223–230.
Schirmer, M., Luster, J., Linde, N., Perona, P., Mitchell, E.A.D., Barry, D.A., Hollender, J., Cirpka, O.A., Schneider, P., Vogt, T., Radny, D., Durisch-Kaiser, E., 2014. Morphological, hydrological, biogeochemical and ecological changes and challenges in river restoration – the Thur River case study. Hydrol. Earth Syst. Sci. 18, 2449–2462.
Schneider, C.A., Rasband, W.S., Eliceiri, K.W., 2012. NIH image to imageJ: 25 years of image analysis. Nat. Methods 9, 671–675.
Schomburg, A., Schilling, O.S., Guenat, C., Schirmer, M., Le Bayon, R.C., Brunner, P., 2018. Topsoil structure stability in a restored floodplain: impacts of fluctuating water levels, soil parameters and ecosystem engineers. Sci. Total Environ. 639, 1610–1622.
Shipitalo, M.J., Nuutinen, V., Butt, K.R., 2004. Interaction of earthworm burrows and cracks in a clayey, subsurface-drained, soil. Appl. Soil Ecol. 26, 209–217.
Shuster, W.D., McDonald, L.P., McCartney, D.A., Parmelee, R.W., Studer, N.S., Stinner, B.R., 2002. Nitrogen source and earthworm abundance affected runoff volume and nutrient loss in a tilled-corn agroecosystem. Biol. Fertil. Soils 35, 320–327.
Singer, M.J., Southard, R.J., Warrington, D.J., Janitzky, P., 1992. Stability of synthetic sand clay aggregates after wetting and drying cycles. Soil Sci. Soc. Am. J. 56, 1843–1848.
Six, J., Elliott, E.T., Paustian, K., 2000. Soil structure and soil organic matter: II. A normalized stability index and the effect of mineralogy. Soil Sci. Soc. Am. J. 64, 1042–1049.
Six, J., Conant, R.T., Paul, E.A., Paustian, K., 2002. Stabilization mechanisms of soil organic matter: implications for C-saturation of soils. Plant Soil 241, 155–176.
Skálová, H., Moravcová, L., Pyšek, P., 2011. Germination dynamics and seedling frost resistance of invasive and native Impatiens species reflect local climatic conditions. Perspect. Plant Ecol. 13, 173–180.
Spiers, G.A., Gagnon, D., Nason, G.E., Packlee, E.C., Lousier, J.D., 1986. Effects and importance of indigenous earthworms on decomposition and nutrient cycling in coastal forest ecosystems. Can. J. For. Res. 16, 983–989.
Strasser, D., Lensing, H.-J., Nuber, T., Richter, D., Frank, S., Goeppert, N., Goldscheider, N., 2015. Improved geohydraulic characterization of river bed sediments based on freeze-core sampling – development and evaluation of a new measurement approach. J. Hydrol. 527, 133–141.
Tanner, C.C., 2001. Plants as ecosystem engineers in subsurface-flow treatment wetlands. Water Sci. Technol. 44, 9–17.
Tisdall, J.M., Oades, J.M., 1982. Organic matter and water-stable aggregates in soils. J. Soil Sci. 33, 141–163.
Tockner, K., Stanford, J.A., 2002. Riverine flood plains: present state and future trends. Environ. Conserv. 29, 308–330.
Turberg, P., Zeimetz, F., Grondin, Y., Elandoy, C., Buttler, A., 2014. Characterization of structural disturbances in peats by X-ray CT-based density determinations. Eur. J. Soil Sci. 65, 613–624.
Velasquez, E., Pelosi, C., Brunet, D., Grimaldi, M., Martins, M., Rendeiro, A.C., Barrios, E., Lavelle, P., 2007. This ped is my ped: visual separation and neat infrared spectra allow determination of the origins of soil macro-aggregates. Pedobiologia 51, 75–87.
Walling, D.E., Collins, A.L., 2016. Fine sediment transport and management. In: River Science: Research and Management for the 21st Century. Wiley-Blackwell (416 pages).
Wickham, H., 2009. ggplot2: Elegant Graphics for Data Analysis. Springer-Verlag New York.
Yavitt, J.B., Fahey, T.J., Sherman, R.E., Groffman, P.M., 2015. Lumbricid earthworm effects on incorporation of root and leaf litter into aggregates in a forest soil, New York State. Biogeochemisty 125, 261–273.
Zaller, J.G., Arnone, J.A., 1999. Earthworm and soil moisture effects on the productivity and structure of grassland communities. Soil Biol. Biochem. 31, 517–523.
Zangerlé, A., Pando, A., Lavelle, P., 2011. Do earthworms and roots cooperate to build soil macro-aggregates? A microcosm experiment. Geoderma 167–68, 303–309.
Zhang, Z.F., Groenevelt, P.H., Parkin, G.W., 1998. The well shape-factor for the measurement of hydraulic properties using the Guelph Permeameter. Soil Tillage Res. 49, 219–221.
Zorn, M.I., van Gerstel, C.A.M., Morrien, E., Wagenaar, M., Eijsackers, H., 2008. Flooding responses of three earthworm species, Allolobophora chlorotica, Aporrectodea caliginosa and Lumbricus rubellus, in a laboratory-controlled environment. Soil Biol. Biochem. 40, 587–593.